

RESEARCH ARTICLE

Effect of Land Use/Land Cover Changes on Land Surface Temperature and Human Thermal Comfort in Greater Karu Urban Area of Nasarawa State, Nigeria

Ishaya S¹, Babatunde Oladipo Lawal², Tochukwu Ikediashi³

^{1,2,3}Department of Geography and Environmental Management, University of Abuja, P.M.B. 117, Abuja, Nigeria.

Received: 12 October 2024 Accepted: 28 October 2024 Published: 29 October 2024

Corresponding Author: Babatunde Oladipo Lawal, Department of Geography and Environmental Management, University of Abuja, P.M.B. 117, Abuja, Nigeria.

Abstract

This study ascertain the effect of land use/land cover Changes on Land Surface Temperature and Human Thermal Comfort in Greater Karu Urban Area of Nigeria. Multi-criteria research design was used to acquire, process and analyse remotely sensed satellite imageries and other related dataset. The remote data used were Landsat TM, Landsat ETM and Landsat OLI that contain Land Surface Temperature data emitted by objects in the study area and stored the information as a digital number (DN). LANDSAT TM images were obtained for 4 different epochs; 1992, 2002, 2012 and 2022. The study used ESRI ArcGIS 10.8, ArcGIS Pro version 3.1.3 and Qgis version 3.22.5 for data acquisition, processing, modelling and analysis. Findings shows that water bodies, cropland and largely vegetal cover area are loss to built-up and bare surface in the GKUA. Findings shows that during the dry season area with low LST (< 200C) and area with moderate LST (>20–23) declining trend, area with high LST (>23-260C) and area with extreme LST (>260C) had increasing trend. During the dry season, area with low LST (< 200C) and area with moderate LST (>20–23) depict declining trend while are with high LST (>23-260C), area with high LST (>23-260C) and area with extreme LST (>260C) had an increasing trend. Substantially during the dry season, there was an increase in DI between 1992-2002 and 2012-2022 in areas with majority of the population anticipated to feel discomfort, area with the entire population feeling thermal discomfort and area with emergency thermal discomfort conditions increased in GKUA. During the wet season thermal DI between 1992-2002 was more in areas where majority of the population are anticipated to have thermal discomfort in GKUA while between 2002-2012 and 2012-2022 majority of the population were anticipated to feel discomfort, area with the entire population feeling thermal discomfort and area with emergency thermal discomfort conditions increased in GKUA. This study recommend urban greening of GKUA.

Keywords: LST, Discomfort, Index, Trend, Change, Detection.

1. Introduction

Concurrently, global climate change has increased the frequency of extreme heatwaves, worsening urban conditions and reducing thermal comfort (Renet *al* 2022). The escalation of Land Surface Temperatures (LST) resulting from land use/land cover changes has invited considerable attention from urban inhabitants and climate scientists. LST's impact is notably pronounced in highly urbanized areas due to

the high ratio of impermeable surfaces (Chen *et al.*, 2023, Adeyeriet *al.*, 2023). Higher LSTs are caused by impervious surfaces, poor urban layout, darker building colour and material, density of urban vegetation and heat-absorbing construction materials used to build urban infrastructures. Impervious surfaces absorb solar radiations creating higher temperatures (Wang, 2015).

In densely built areas, a poor layout can give rise to the 'canyon effect' where airflow is hindered and

Citation: Ishaya S., Babatunde Oladipo Lawal, Tochukwu Ikediashi. Effect of Land Use/Land Cover Changes on Land Surface Temperature and Human Thermal Comfort in Greater Karu Urban Area of Nasarawa State, Nigeria. *Annals of Ecology and Environmental Science*. 2024; 6(2):41-55.

©The Author(s) 2024. This is an open access article distributed under the Creative Commons Attribution License, which permits unrestricted use, distribution, and reproduction in any medium, provided the original work is properly cited.

heat trapped, creating higher temperatures (Thaniet *al* 2013). Dark building colours and non-reflecting building surfaces also produce higher temperatures (Olubukola *et al.*, 2023). The conversion of natural surfaces into built form due to urban development and LULC changes contribute to higher temperatures (Ishaya and Areo, 2018; Zhang and Liang, 2019) and the removal of vegetation reduces evapotranspiration, leading to less cooling effect through latent heat exchange and consequently higher land surface temperatures leading to human discomfort.

Urban areas typically have higher temperatures compared to surrounding rural areas due to increased heat retention by buildings, roads, and other infrastructure, as well as reduced vegetation cover. This can significantly impact human thermal comfort, especially during heatwaves (Hou and Murayama, 2019). LSTs can be measured by different sensors. Over the years, Greater Karu Urban Area has been experiencing expansion of built-up areas which have the tendencies to contribute to LST and in the long run stimulates urban thermal discomfort. In line with these, it is of importance to ascertain the effect of land use/land cover changes on land surface temperature and human thermal comfort in Greater Karu Urban Area of Nasarawa State given its area size of 722 km² and a population of over two million and being one of the fastest growing urban areas in the world, with a growth rate of 40 percent recorded annually (Rikko and Laka, 2013).

2. Study Methodology

2.1 Study Area

Greater Karu Urban Area (GKUA) approximately

located between latitudes 8° 5'N and 9° 25'E and longitudes 7° 54'E and 10° 42'N East of the Greenwich Meridian. It extends from the eastern boundary of the Federal Capital Territory Abuja, (Old Nyanya) to Gora about 15 kilometers to Keffi. The planning area shares common boundaries with the Federal Capital Territory (FCT) Abuja to the west, Keffi Local Government Area (LGA) to the south, Nasarawa LGA and Jaba Local Government Area of Kaduna state to the north, (see details in figures 3.1 and 3.2). GKUA has both urban and rural settlements. The major urban settlements comprising of Mararaba, New Karu, New Nyanya, Masaka and Uke as well as rural areas that have been overtaken by new urban development and engulfed by the larger ones such as Zhenwu, Luvu, Kuchikau, Kodepe, AsoPada, Ado, Koroduma and One-Man Village ((Laka, 2013). It has an area of 722 km² and a population of some 2 million (Rikko and Laka, 2013).

The average temperature of the study area is 29°C. The study area had an average rainfall of 1250mm and an average wind speed of 9 km/h is recorded for the study area (Rikko and Laka, 2013). Tropical ferruginous soils make up the major soil units found in the study area. The parent material for the soils are from basement complex and sedimentary formations in the area. Laterite crust occurs extensively on the basement complex rocks while hydromorphic soils are common along river Benue trough and flood plains of major rivers (Auduet *al.*, 2018). The natural vegetation is of the park savannah type, featuring dense tropical woodland with shrubs and grasses (Udeh, 2010).

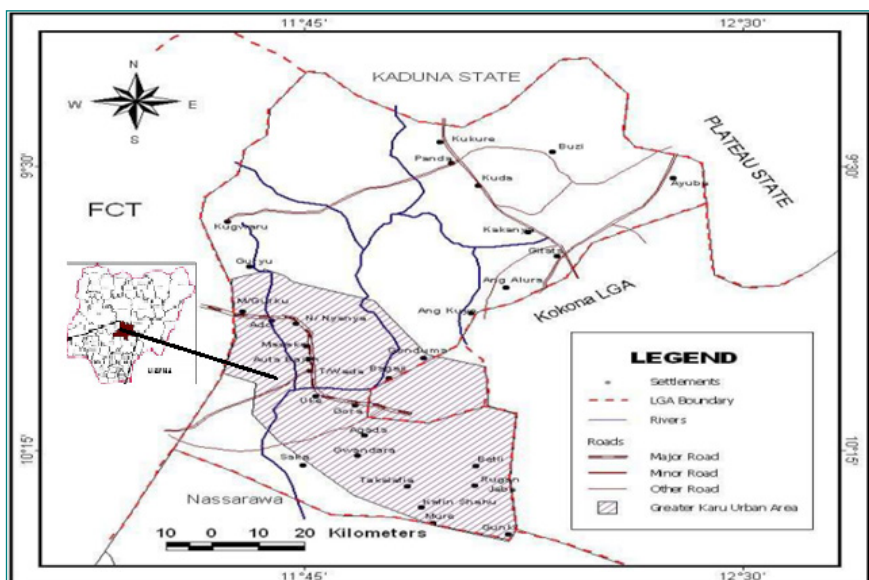


Figure 1. Karu LGA showing the study area (GKUA) Source: Adapted from Rikko (2013)

2.2 Research Design, Data and Software’s Used

Multi-criteria research design was used to acquire, process and analyse remotely sensed satellite imageries and other related dataset. The remote data used were Landsat TM, Landsat ETM and Landsat OLI that contain Land Surface Temperature data

emitted by objects in the study area and stored the information as a digital number (DN). LANDSAT TM images were obtained for 4 different epochs; 1992, 2002, 2012 and 2022. The study used ESRI ArcGIS 10.8, ArcGIS Pro version 3.1.3 and Qgis version 3.22.5 for data acquisition, processing, modelling and analysis.

Table 1. Images used in the study

S/No.	Study Area	Path/Row	Satellite Date of Acquisition	Satellite Sensor I.D	Bands	Resolution (m)
	GKUA	188/54	1992	Landsat 4 Thematic Mapper (TM)	2-5,7	30
					6	60
			2002 and 2012	Landsat 7 Enhanced Thematic Mapper Plus (ETM+)	2-5,7	30
					6	60
			2022	Landsat 8 OLI/TIRS	2 -7	30
					10	30
			2022	ASTER (GDEM)	-	1-arc seconds

Source: Researcher Compilation, 2024.

2.3 Image Pre-processing

QGIS 3.22.5 software was used for gap filling. Atmospheric correction was performed to remove the effects of solar illumination differences and other atmospheric anomalies (like atmospheric path reflectance, electromagnetic scattering/absorption) from the imageries. Using Available Band List Module in Qgis, false colour Bands were combined to form an Image. The Bands were 432 in which vegetation appears red in colour, water appears cyan and bare surface appears white. The study area was subset by masking out all areas not falling within the study area. This was done by overlaying a vector shape file on the raster image and assigning values of 1 to the area of interest and 0 to the rest of the image respectively (Imran *et al.*, 2022).

2.3.1 Classification Accuracy

Kappa statistic was used in classification accuracy. Kappa values are characterized as <0 as indicative of no agreements and 0–0.2 as slight, 0.2–0.41 as fair, 0.41–0.60 as moderate, 0.60–0.80 as substantial and 0.81–1.0 as almost perfect agreement (Imran *et al.*, 2022). Accuracy assessment tasks was performed on the 1992, 2002, 2012 and 2022 imageries. The classification accuracy calculates the statistics of percentages of accuracy relative to error matrix results. The error matrix compares the historical values to the assigned class values. Kappa statistics measures the ability to provide information about a single matrix as well as to compare matrices (Himanshu and Subhanil, 2021).

2.4 Image Processing Stage

Image processing include extraction of NDVI, estimation of Land Surface Temperature (LST) and Land Use/Land Cover (LU/LC) Analysis.

2.4.1 Extraction of NDVI

Normalized Differential Vegetation index (NDVI) was generated using near infrared band and red band i.e. band 4 and 3 in Landsat TM and ETM+ and bands 5 and 4 in Landsat 8 OLI/TIR. The NDVI was used as indicator of vegetation density in the study area. This was done using the NDVI equation below:

$$NDVI = (NIR \text{ Band} - RED \text{ Band}) / (NIR \text{ Band} + RED \text{ Band}).$$

2.4.2 Estimation of Land Surface Temperature

To estimate the LST from the pre-processed Landsat images, the temperature data stored as DN values in the thermal band 10 (low gain band) for ETM+ and band 6 for TM was converted to spectral radiance values using the following standard LMin and LMax spectral radiance scaling factors equation (NASA, 2011):

$$Radiance = L_{Max\lambda} - L_{min\lambda} * QCAL - QCAL_{MIN} + L_{min\lambda}$$

$$QCAL_{Max} - QCAL_{Min} \text{ -----}. \quad (i)$$

Where: QCAL = digital number

L_{MIN}λ = spectral radiance scales to QCAL_{MIN}

L_{MAX}λ = spectral radiance scales to QCAL_{MAX}

QCALMIN = minimum quantized calibrated pixel value (usually = 1)

QCALMAX = maximum quantized calibrated pixel value (usually = 255)

The scene calibration data were available on the metadata file of each Landsat scene. Having computed the spectral radiance values for each of the Landsat scenes, were subsequently converted to temperature values (Kelvin) using the inverse of the Planck function shown below:

$$T = K2 / \ln[K1 * E / \text{Radiance} + 1] \dots \dots \dots (ii)$$

Where: T = Effective at-satellite temperature in Kelvin

K2 = Calibration constant 2

K1 = Calibration constant 1

ϵ = Emissivity (typically 0.95)

Radiance = Spectral radiance

2.4.3 Land Use Land Cover Analysis

Land use/Land cover analysis was carried out using ArcGis Pro software. Bands 1, 2, 3, 4, 5 and 7 (for Landsat 5 and 7), and bands 2, 3, 4, 5, 6, and 7 (for Landsat 8) was stacked together to form a single image for each of the years under study. Supervised classification was used to classify the images in order to make terrestrial materials identifiable based on their spectral signatures and characteristics. In this case, the Maximum Likelihood Algorithm was used.

$$P(x|C_j) = \frac{1}{(2\pi)^{n/2} |\Sigma_c|^{1/2}} \exp\left(-\frac{1}{2}(x - \mu_c)^T \Sigma_c^{-1} (x - \mu_c)\right) \dots \dots (ii)$$

Where:

X is the spectral vector of the pixel (i.e., the set of values for different bands or features).

C_j = denotes the class j.

μ_c = the mean vector of class j.

Σ_c = the covariance matrix of class j.

K = the number of bands (features) in the data.

| Σ_c | = the determinant of the covariance matrix

2.4.4 Calculation of Human Thermal Comfort

Following Giannarose *et al.* (2014), this study examined two bio-meteorological indices to characterize HTC: (a) the Discomfort Index (DI) and (b) the Approximated Wet-bulb Globe Temperature (AWBGT). The key variable in calculating the DI and AWBGT was the air

temperature or LST. Giannarose *et al.* (2014) considered these straightforward indices as they are widely used indices of thermal comfort and validated by the existing observational data. These two indices were used in calculating HTC in the GKUA. Furthermore, air temperature was replaced with LST for calculating the HTC at land surface level.

The extensively used DI index suggested by Thom (1959) to express thermal comfort as also used in this study thus:

$$DI = Ta - 0.55 \times (1 - 0.01 \times RH) \times (Ta - 14.5) \dots (iii)$$

The Ta denotes air temperature (⁰C), while RH denotes the relative humidity (%). This study calculates DI using LST rather than Ta since only LST is calculated from remote sensing data.

HTC was calculated at the pedestrian level (Zhang, *et al.*, 2020; Toy and Kantor, 2017). This study estimated the outdoor HTC at a surface level using LST to understand the effect of LULC changes on the HTC. To this end, a further HTC index AWBGT was calculated using Equation (4) developed by Steeneveld *et al.* (2011).

$$AWBGT = 0.567 \times Ta + 0.393 \times e + 3.94 \dots (iv)$$

Here, Ta is air temperature (⁰C) and e is water vapor pressure (hPa), but LST was used in this case instead of Ta. Saturation water vapor pressure was calculated using the Goff-gratch equation (Eq. 5). Then, using saturation water vapor pressure and relative humidity, the vapor pressure was calculated.

$$\log_{10} e_w = -7.90298 \left(\frac{T_{st}}{T} - 1\right) + 5.02808 \log_{10} \left(\frac{T_{st}}{T}\right) - 1.3816 \\ \times 10^{-7} \left(10^{11.344 \left(1 - \frac{T_{st}}{T}\right)} - 1\right) + 8.1328 \times 10^{-3} \left(10^{-3.49149 \left(\frac{T_{st}}{T} - 1\right)} - 1\right) + \log_{10} e_{st} \dots \dots (v)$$

Here, e_w denotes the saturation water vapor pressure (hPa), T_{st} denotes the steam point temperature (373.15 K), T denotes the absolute air temperature (K), and e_{st} denotes the steam-point pressure (1013.25 hPa).

3. Result and Discussion

3.1 Land Use/Land Cover Accuracy Assessment

The Land use/Land cover results revealed that, the overall classification accuracy of the imageries produced almost perfect Kappa statistics of 86.7% in 1992, 91.6% in 2002, 92.1% in 2012, and 83.5% in 2022. Results for all the study years were above 80%

Keppa statistics indicating classification accuracy of almost perfect agreement as observed by Lee, *et al.* (2021).

3.1.1 Land Use/Land Cover Characterization and Changes from 1992 to 2022

The LULC characteristics of GKUA in the year 1992 shows that cropland class dominated the landscape with 346.7km² (48.0%), vegetal cover had 196.8km² (27.2%), bare surface covered 168.9km² (23.4%), built-up area had 3.1km² (1.3%) and the least was water bodies with an area coverage of 1.4km² (0.2%). In the year 2002, cropland class also dominated the landscape with 403.6km² (55.8%), bare surface covered 164.4km² (22.7%), vegetal cover covered

131.2km² (18.1%), built-up area covered 22.1km² (3.1%) while the least was water bodies with area coverage of 1.6km² (0.221%). In 2012, cropland covered 304.7km² (42.1%), bare surface covered 200.5km² (27.7%), vegetation covered an area of 149.6km² (20.7%), built-up had an area coverage of 65.2 km² (9.0%) while water bodies was 2.9km² (0.401%) of the total area. In 2022, cropland covered 307.8km² (42.6%), bare surface covered 255.3km² (35.3%), built-up had an area coverage of 153.4km² (21.2%), vegetation covered an area of 3.9km² (0.5%), while water bodies was 2.5km² (0.346%) of the total area (See Figure 2 and Table 2).

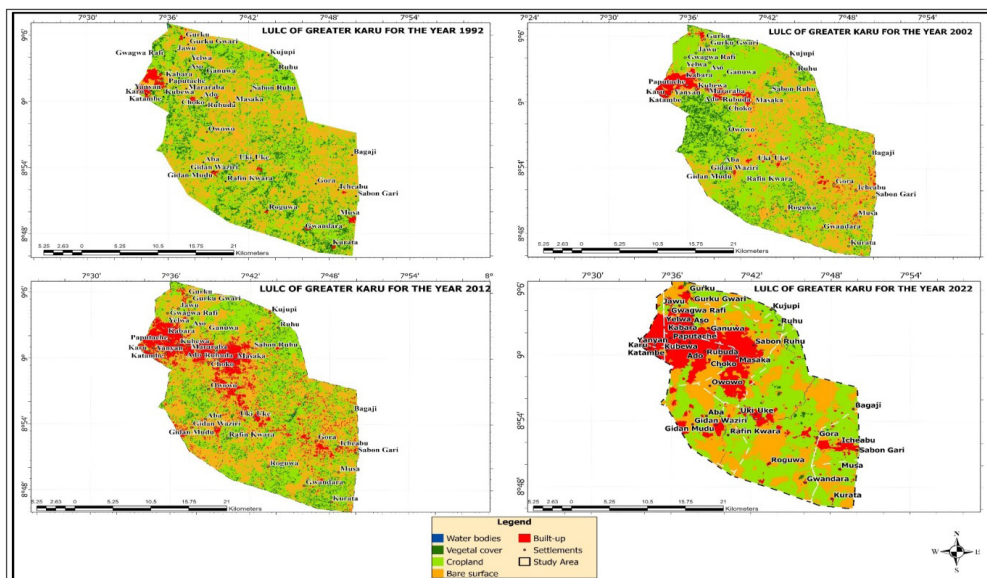


Figure 2. Land Use/Land Cover Characterization for the year 2022

Table 2. Land Use/Land Cover Classification of GKUA from 1992 -2022

1992		
Classes	Area SqKm	%
Water bodies	1.4	0.2
Vegetal cover	196.8	27.2
Cropland	346.7	48.0
Bare surface	168.9	23.4
Built-up	9.1	1.3
Total	722.9	100
2002		
Classes	Area SqKm	%
Water bodies	1.6	0.221
Vegetal cover	131.2	18.1
Cropland	403.6	55.8
Bare surface	164.4	22.7
Built-up	22.1	3.1
Total	722.9	100

2012		
Classes	Area SqKm	%
Water bodies	2.9	0.401
Vegetal cover	149.6	20.7
Cropland	304.7	42.1
Bare surface	200.5	27.7
Built-up	65.2	9.0
Total	722.9	100
2022		
Classes	Area SqKm	%
Water bodies	2.5	0.346
Vegetal cover	3.9	0.5
Cropland	307.8	42.6
Bare surface	255.3	35.3
Built-up	153.4	21.2
Total	722.9	100

Source: Researcher Analysis, 2024.

3.1.2 Change Detection of LU/LC from 1992 to 2022 in GKUA

Table 3 depicts LU/LC changes between 1992 to 2022 in GKUA with water bodies area coverage increased with 0.2km² (0.03%) from 1992 to 2002, from 2002-2012 it had an increased value of 1.3km² (0.18%) and from 2012 to 2022 had decreased value of 0.40 (0.06%). The pattern of changes in cropland area coverage shows that between 1992 to 2002 there was an increase of 56.9 km² (7.87%), but a decrease of -98.9km² (-13.68%) was observed from 2002-2012 while from 2012-2022 an increase of 3.10km² (0.43%) was observed. The distribution of vegetal

coverage in GKUA shows a decrease of -65.6km² (-9.07%) but depicts an increase of 18.4km² (2.55%) between 2002 to 2012 and also a pronounced decrease of -145.70km² (-20.15%) between 2012-2022. Over the study period built-up area have been in consistent increase from 1992 to 2022 with built up area increase of 13.0 km² (1.8%), an increase of 43.1 km² (5.96%) from 2002 to 2012 and a tremendous increase of 88.20km²(12.2%) from 2012 to 2022. Bare surface decrease with -4.5km² (-0.62%) from 1992 to 2002, from 2002 to 2012 it increase with 36.1 km² (4.99%), between 2012 to 2024 bare surface increase with 54.8km² (7.58%).

Table 3. Change Detection of LU/LC from 1992 to 2022 in GKUA

Classes	1992 - 2002		2002 - 2012		2012 - 2022		1992 - 2022	
	Changes (Km ²)	%	Changes (Km ²)	%	Changes (Km ²)	%	Changes (Km ²)	%
Water bodies	0.2	0.03	1.3	0.18	-0.40	-0.06	1.1	0.2
Cropland	56.9	7.87	-98.9	-13.68	3.10	0.43	-38.9	-5.4
Vegetal cover	-65.6	-9.07	18.4	2.55	-145.70	-20.15	-192.9	-26.7
Built-up	13.0	1.80	43.1	5.96	88.20	12.20	144.3	20.0
Bare surface	-4.5	-0.62	36.1	4.99	54.80	7.58	86.4	12.0

Source: Researcher Analysis, 2024.

Generally from 1992 to 2022, water bodies increase with 1.1km² (0.2%), cropland decrease with -38.9 (-5.4%), vegetal cover decrease with -192.9 (-26.7%), built-up area increase with 144.3Km² (20%), bare surface also increase with 86.4Km²(12.2%) (Table 3). Cropland and vegetal cover experienced more of the decrease while built-up and bare surface experienced more of the increase in change in the GKUA over the

period. This is due to consistent housing demands by workers and economic prospect seekers in the Federal Capital City (FCC) of the Federal Capital Territory of Nigeria who can't afford accommodation with the FCC. The demolition of slums within the FCC force low income earners to move into Greater Karu Urban Areas and commutes to work in the FCC during the working days of the week. The findings

in GKUA aligned with the observations of Kumar and Sangwan (2013) that land use changes is more of increase in built-up area and bare surface but with decrease in vegetal and agricultural land. Ade and Afolabi (2013) findings of change detection in the Federal Capital Territory of Nigeria from 1987-2007; Balogun *et al.*, (2011) observed urban expansion and land use changes in Akure. Ejaro and Abdullahi (2013) observed also increase in built-up area and bare surface with decrease in vegetal cover and agricultural land. In GKUA, the ever-increasing population, migration and changing functions of urban areas as caused by urbanization leads to land use changes turn affecting land use/land cover. Choudhury *et al.*, (2019) observed that this situation could lead to problems of environmental degradation and shortage of land for agriculture, water resources depreciation and overall ecosystem service depreciation.

3.2 Land Surface Temperature of Greater (LST) GKUA from 1992 to 2022

The Land Surface Temperature of Greater (LST) GKUA from 1992 to 2022 are presented for dry and wet season for the years 1992, 2002, 2012 and 2022.

3.2.1 Dry Season LST of GKUA from 1992 to 2022

Table 4 presents the LST values during the dry season

Table 4. Dry and Wet Season LST of GKUA from 1992 to 2022

Dry Season LST of GKUA in 1992			Wet Season LST of GKUA in 1992	
Classes	Area (Km ²)	Percentage	Area (Km ²)	Percentage
< 20	204.5	28.3	204.4	28.3
> 20 - 23	371.8	51.4	371.8	51.4
> 23 - 26	120.2	16.6	120.2	16.6
> 26	26.4	3.7	26.5	3.7
Total	722.9	100	722.9	100
Dry Season LST of GKUA in 2002			Wet Season LST of GKUA in 2002	
Classes	Area (Km ²)	Percentage	Area (Km ²)	Percentage
< 20	28.1	3.9	153.0	21.2
> 20 - 23	132.4	18.3	317.4	43.9
> 23 - 26	347.2	48.0	207.6	28.7
>26	215.2	29.8	44.9	6.2
Total	722.9	100	722.9	100
Dry Season LST of GKUA in 2012			Wet Season LST of GKUA in 2012	
Classes	Area (Km ²)	Percentage	Area (Km ²)	Percentage
< 20	44.9	6.2	66.4	9.2
> 20 - 23	222.2	30.7	132.4	18.3
> 23 - 26	318.7	44.1	317.7	43.9
> 26	137.1	19.0	206.4	28.5
Total	722.9	100	722.9	100

for different LU/LC classes in the GKUA from 1992 to 2022. In the year 1992, wet season LST varies over space with area having low LST ($\leq 20^{\circ}\text{C}$) covering 3.9% of the study area, area with moderate LST ($>20^{\circ}\text{C}-23^{\circ}\text{C}$) covered 18.3%, area with high LST ($>23^{\circ}\text{C}-26^{\circ}\text{C}$) covered 48.0% while area with extreme LST ($>26^{\circ}\text{C}$) covered 29.8% of the GKUA. In the year 2002 dry season, low LST ($\leq 20^{\circ}\text{C}$) area occupied 3.9% of the total area, area with moderate LST ($>20^{\circ}\text{C}-23^{\circ}\text{C}$) covered 18.3% of the study area, area with high LST ($>23^{\circ}\text{C}-26^{\circ}\text{C}$) covered 48.0% of the study area while area with extreme LST ($>26^{\circ}\text{C}$) covered 29.8% of the GKUA. LST result in the dry season of 2012, shows that area that had low LST ($\leq 20^{\circ}\text{C}$) covered 6.2% of the study area, area with moderate LST ($>20^{\circ}\text{C}-23^{\circ}\text{C}$) dominate 30.7% of the study area, area with high LST ($>23^{\circ}\text{C}-26^{\circ}\text{C}$) covered 44.1% of the study area while area with extreme LST ($>26^{\circ}\text{C}$) covered 19.0% of the study area. In 2022, low LST ($\leq 20^{\circ}\text{C}$) area occupied 6.2% of GKUA, area with moderate LST ($>20^{\circ}\text{C}-23^{\circ}\text{C}$) covered 26.9% of GKUA, area with high LST ($>23^{\circ}\text{C}-26^{\circ}\text{C}$) covered 28.0% of the study area while area with extreme LST ($>26^{\circ}\text{C}$) covered 38.9% of the GKUA (See Table 4 and Figure 3).

Dry Season LST of GKUA in 2022			Wet Season LST of GKUA in 2022	
Classes	Area (Km ²)	Percentage	Area (Km ²)	Percentage
< 20	44.6	6.2	44.6	6.2
> 20 - 23	194.6	26.9	194.5	26.9
> 23 - 26	202.2	28.0	202.2	28.0
> 26	281.5	38.9	281.6	39.0
Total	722.9	100	722.9	100

Source: Researcher Analysis 2024

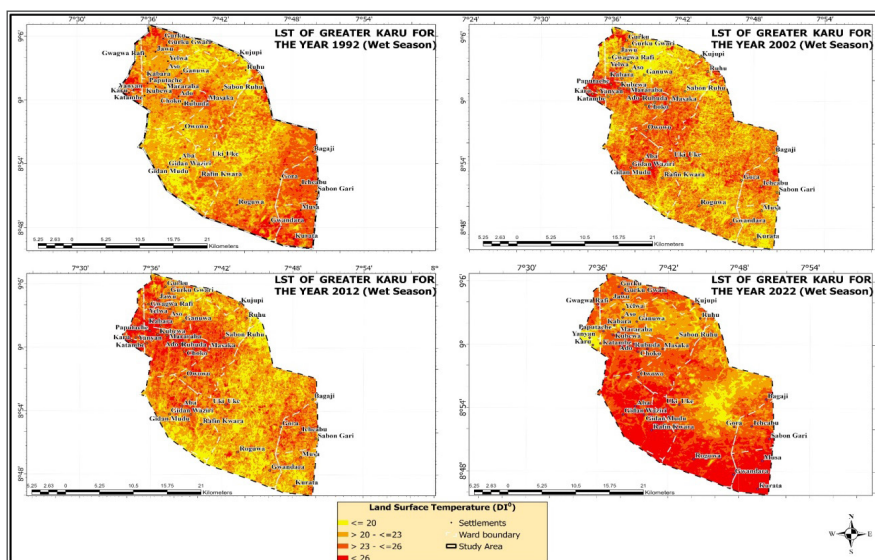


Figure 3. Dry Season LST of GKUA from 1992 to 2022

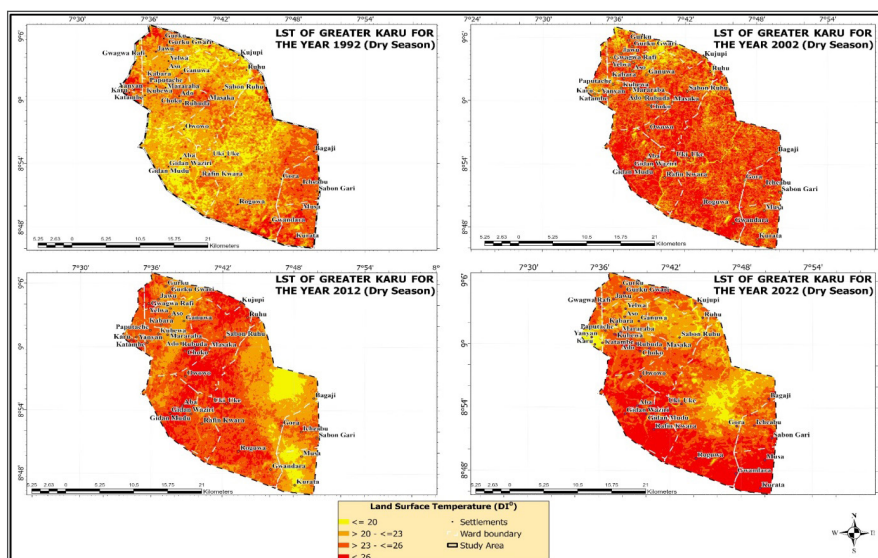


Figure 4. Wet Season LST of GKUA from 1992 to 2022

3.2.2 Wet Season LST of GKUA from 1992 to 2022

Table 3 and Figure 4 presents the LST values during the wet season for different LU/LC classes in the GKUA from 1992 to 2022. In the year 1992, wet season LST varies over space with area having low LST $\leq 20^{\circ}\text{C}$ covering 28.3% of the study area, area with moderate LST ($>20^{\circ}\text{C}$ - 23°C) covered 51.4% of the study area, area with high LST ($>23^{\circ}\text{C}$ - 26°C) covered 16.6% of the study area while area with extreme LST ($>26^{\circ}\text{C}$)

covered 3.7% of the GKUA. In the year 2002 wet season, low LST $\leq 20^{\circ}\text{C}$ area occupied 21.2% of the study area, area with moderate LST ($>20^{\circ}\text{C}$ - 23°C) covered 43.9% of the study area, area with high LST ($>23^{\circ}\text{C}$ - 26°C) covered 28.7% of the study area while area with extreme LST ($>26^{\circ}\text{C}$) covering 6.2% of the GKUA. LST result in the wet season of 2012, shows that area that had low LST $\leq 20^{\circ}\text{C}$ covered 6.2% of the total area, area with moderate LST ($>20^{\circ}\text{C}$ - 23°C)

dominating 30.7% of the study area, area with high LST ($>23^{\circ}\text{C}$ - 26°C) covered 44.1% of the area while area with extreme LST ($>26^{\circ}\text{C}$) covering 19.0% of the study area. During the wet season in the year 2022, low LST ($\leq 20^{\circ}\text{C}$) area occupied 9.2% of GKUA, area with moderate LST ($>20^{\circ}\text{C}$ - 23°C) covered 18.3% of GKUA, area with high LST ($>23^{\circ}\text{C}$ - 26°C) covered 43.9% of the study area while area with extreme LST ($>26^{\circ}\text{C}$) covered 28.5% of the GKUA (See Table 3 and Figure 4). Findings clearly portrays increase in areas with high LST ($>23^{\circ}\text{C}$ - 26°C) and area with extreme LST ($>26^{\circ}\text{C}$) for both dry season which is in line with the findings of Chen *et al.*, (2023) where he unveil a relationship between urban spatial form and seasonal land surface temperature under different grid scales. Similar the observation of Mumtaz *et al.*, (2020) in modeling spatio-temporal land transformation and its associated impacts on land surface temperature (LST). Also Adakayi and Ishaya (2016) and Ishaya (2020) had similar observations.

3.3 Discomfort Index in Greater Karu Urban Area from 1992-2022

The discomfort index which is the measure of how uncomfortable or oppressive weather conditions feel to humans, particularly in terms of heat and humidity was carried out for both wet and dry season in the GKUA for 1992, 2002, 2012 and 2022.

3.3.1 Dry Season Discomfort Index in Greater Karu Urban Area in 1992

The dry season is characterized by low relative humidity and typically higher temperatures, which can lead to different perceptions of discomfort compared to the humid conditions of the wet season. In 1992, Table 5 and Figure 5 shows that area with $<21^{\circ}\text{C}$ discomfort index covered 54.0 km² (7.5%) in area having all its inhabitants experiencing no thermal discomfort, area with $21-24^{\circ}\text{C}$ covered 186.8 km² (25.8%) in locations having less than half of the population expected to feel thermal discomfort. Area with $24-27^{\circ}\text{C}$ covered 249.3 km² (34.5%) of locations with 50% of the population feeling discomfort, area with $27-29^{\circ}\text{C}$ covered 143.3 km² (19.8%) of area that will have majority of the population anticipated to feel discomfort while area with $29-32^{\circ}\text{C}$ covered 60.7 km² (8.4%) of locations expected that entire population will feel thermal discomfort and area with $>32^{\circ}\text{C}$ covering 28.8 km² (4.0%) of locations that depicts emergency thermal discomfort conditions for all inhabitants.

Dry Season Discomfort Index of Greater Karu Urban Area in 2002

In 2002 dry season, the discomfort index values in GKUA shows that $<21^{\circ}\text{C}$ covered 14.1 km² (1.9%) of area with all its inhabitants experiencing no thermal discomfort, $21-24^{\circ}\text{C}$ covered 44.5 km² (6.2%) area with less than half of the population living in this area are expected to feel thermal discomfort, $24-27^{\circ}\text{C}$ covered 156.8 km² (22.1%) area with up to 50% of the population feeling discomfort. It was observed that $27-29^{\circ}\text{C}$ covered 292.4 km² (40.4%) area with majority of the population living in the area anticipated to feel discomfort, $29-32^{\circ}\text{C}$ covered 182.4 km² (25.2%) area with the entire population feeling thermal discomfort while $>32^{\circ}\text{C}$ covered 32.8 km² (4.5%) area that depicts emergency thermal discomfort conditions for all inhabitants (See Table 5 and Figure 5).

Dry Season Discomfort Index of Greater Karu Urban Area in 2012

The discomfort index values for the dry season in the GKUA for the year 2012 shows that $<21^{\circ}\text{C}$ covered 31.8 km² (4.4%) area with its inhabitants experiencing no thermal discomfort, $21-24^{\circ}\text{C}$ covered 110.1 km² (15.2%) area with less than half of the population expected to feel thermal discomfort. $24-27^{\circ}\text{C}$ covered 180.9 km² (25.0%) area indicating up to 50% of the population feeling discomfort. $27-29^{\circ}\text{C}$ covered 263.0 km² (36.4%) of the area with majority of the population anticipated to feel discomfort, $29-32^{\circ}\text{C}$ covered 137.0 km² (18.9%) area with entire population feeling thermal discomfort while $>32^{\circ}\text{C}$ covered 0.1 km² (0.0%) area with emergency thermal discomfort conditions for all inhabitants (Table 5 and Figure 5).

Dry Season Discomfort Index of Greater Karu Urban Area in 2022

In 2022 dry season, the discomfort index values in GKUA shows that $<21^{\circ}\text{C}$ covered 1.1 km² (0.2%) area with all its inhabitants experiencing no thermal discomfort, $21-24^{\circ}\text{C}$ covered 4.4 km² (0.6%) area with less than half of the population expected to feel thermal discomfort. It was observed that $24-27^{\circ}\text{C}$ covered 94.7 km² (13.1%) area with up to 50% of the population feeling discomfort. $27-29^{\circ}\text{C}$ covered 235.9 km² (32.6%) area with majority of the population anticipated to feel discomfort, $29-32^{\circ}\text{C}$ covered 251.9 km² (34.8%) area with the entire population feeling thermal discomfort while $>32^{\circ}\text{C}$ covered 134.9 km² (18.7%) area with emergency thermal discomfort conditions for all inhabitants (See Table 5 and Figure 5).

Table 5. Dry Season Discomfort Index (DI) of GKUA from 1992 - 2022

Dry Season Discomfort Index (DI)			Wet Season Discomfort Index (DI)	
DI (°C) 1992	Area Km ²	Percentage	Area Km ²	Percentage
<21	54.0	7.5	55.3	7.7
21 - 24	186.8	25.8	191.0	26.4
24 - 27	249.3	34.5	254.7	35.2
27 - 29	143.3	19.8	132.8	18.4
29 - 32	60.7	8.4	62.1	8.6
>32	28.8	4.0	27.0	3.7
Total	722.9	100	722.9	100
DI (°C) 2002	Area Km ²	Percentage	Area Km ²	Percentage
<21	14.1	1.9	64.0	8.9
21 - 24	44.5	6.2	172.9	23.9
24 - 27	156.8	21.7	233.4	32.3
27 - 29	292.4	40.4	180.8	25.0
29 - 32	182.4	25.2	60.3	8.3
>32	32.8	4.5	11.4	1.6
Total	722.9	100	722.9	100
DI (°C) 2012	Area Km ²	Percentage	Area Km ²	Percentage
<21	31.8	4.4	52.2	7.2
21 - 24	110.1	15.2	160.1	22.1
24 - 27	180.9	25.0	190.8	26.4
27 - 29	263.0	36.4	168.4	23.3
29 - 32	137.0	18.9	118.1	16.3
>32	0.1	0.0	33.3	4.6
Total	722.9	100	722.9	100
DI (°C) 2022	Area Km ²	Percentage	Area Km ²	Percentage
<21	1.1	0.2	1.7	0.2
21 - 24	4.4	0.6	7.6	1.1
24 - 27	94.7	13.1	116.3	16.1
27 - 29	235.9	32.6	285.6	39.5
29 - 32	251.9	34.8	241.8	33.5
>32	134.9	18.7	69.8	9.6
Total	722.9	100	722.9	100

Source: Researcher Analysis, 2024.

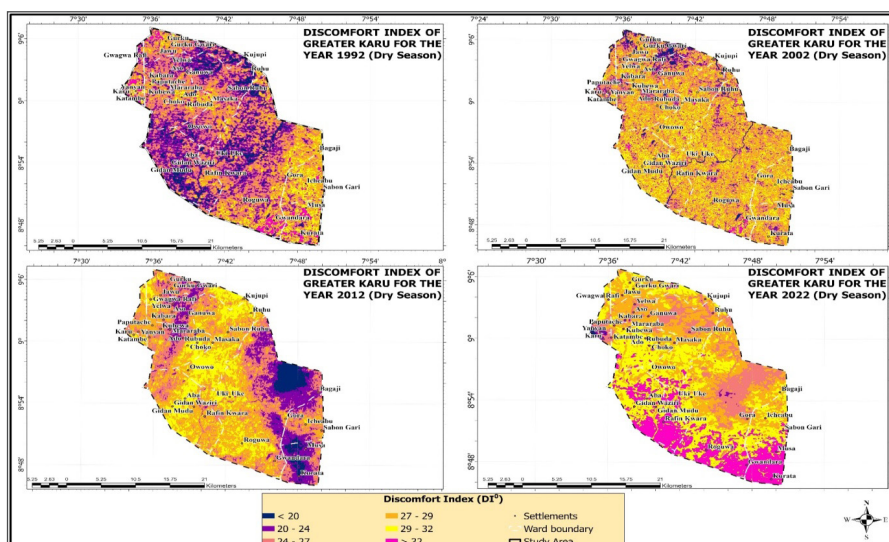


Figure 5. Dry Season Discomfort Index for Greater Karu Urban Area from 1992 - 2022

3.3.2 Wet Season Discomfort Index of Greater Karu Urban Area from 1992-2022

The wet season is characterized by higher relative humidity and typically higher rainfall, which can lead to different perceptions of discomfort compared to the dry season.

Wet Season Discomfort Index of Greater Karu Urban Area in 1992

Table 5 and Figure 6 depicts discomfort index values for wet season in GKUA for the year 1992. The discomfort index shows that <math><21^{\circ}\text{C}</math> covered 55.3km² (7.7%) area with all the inhabitants experiencing no thermal discomfort, 21-24^oC covered 191.0km² (26.8%) area with less than half of the population expected to feel thermal discomfort. It was observed that 24-27^oC covered 254.7km² (35.2%) area with up to 50% of the population feeling discomfort. 27-29^oC covered 132.8km² (18.4%) area with majority of the population anticipated to feel discomfort. 29-32^oC covered 62.1km² (8.6%) of area with the entire population feeling thermal discomfort while area with >32^oC covered 27.0km² (3.7%) area with emergency thermal discomfort conditions for all inhabitants.

Wet Season Discomfort Index of Greater Karu Urban Area in 2002

In the wet season of the year 2002, the discomfort index values in GKUA shows that area with <math><21^{\circ}\text{C}</math> covered 64.0km² (8.9%) area with inhabitants experiencing no thermal discomfort, 21-24^oC that covered 172.9km² (23.9%) area with less than half of the population expected to feel thermal discomfort. 24-27^oC covered 233.4km² (32.3%) area with up to 50% of the population feeling discomfort, 27-29^oC covered 180.8km² (25.0%) area with majority of the population anticipated to feel discomfort. It was observed that 29-32^oC covered 60.3km² (8.3%) area with the entire population experiencing thermal discomfort while

area with >32^oC covered 11.4km² (1.6%) area with depicting emergency thermal discomfort conditions for all inhabitants (See Table 5 and Figure 6).

Wet Season Discomfort Index of Greater Karu Urban Area in 2012

The discomfort index values for the wet season in the GKUA for the year 2012 shows that area with <math><21^{\circ}\text{C}</math> covered 52.2 km² (7.2%) area with all inhabitants experiencing no thermal discomfort. 21-24^oC covered 160.1km² (22.1%) area with less than half of the population expected to feel thermal discomfort, 24-27^oC covered 190.8km² (26.4%) with up to of the inhabitants feeling discomfort. 27-29^oC that covered 168.4km² (23.3%) area with majority of the population living in the area anticipated to feel discomfort, 29-32^oC covered 118.1km² (16.3%) area with the entire population having thermal discomfort while area with >32^oC covered 33.3km² (4.6%) of area with emergency conditions for all inhabitants (Table 5 and Figure 6).

Wet Season Discomfort Index of Greater Karu Urban Area in 2022

The wet season of 2022 discomfort index values in GKUA shows area with <math><21^{\circ}\text{C}</math> covered 1.7 Km² (0.2%) area with all its inhabitants experiencing no thermal discomfort, 21-24^oC covered 7.6 Km² (1.1%) area with less than half of the population living in the area expected to feel thermal discomfort. 24-27^oC covered 116.3km² (16.1%) area with up to 50% of the population feeling discomfort. It was observed that area with 27-29^oC covered 285.6km² (39.5%) area with majority of the population anticipated to feel thermal discomfort, 29-32^oC covered 241.8km² (33.5%) area with the entire population feeling thermal discomfort while >32^oC covered 69.8km² (9.6%) area with that depicts emergency conditions for all inhabitants (See Table 5 and Figure 6).

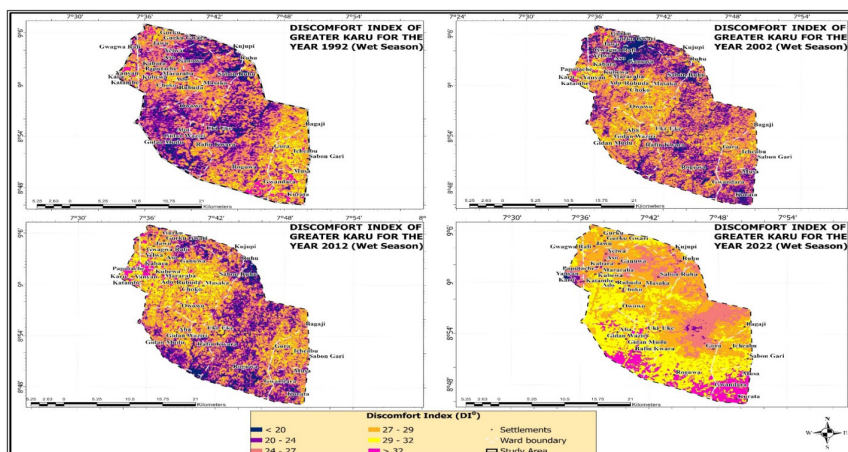


Figure 6. Wet Season Discomfort Index for Greater Karu Urban Area from 1992 - 2022

3.3.3 Discomfort Index Change Detection from 1992 to 2022 in GKUA

Changes in the Discomfort Index indicate shifts in weather patterns that affect human comfort levels and potentially impact health and productivity in GKUA.

Dry Season Discomfort Index Change Detection from 1992 to 2022 in GKUA

During the dry season between 1992-2002 area with no thermal discomfort (<21°C), area with less than half of the population feeling thermal discomfort (21 °C to 24°C) as well as area with 50% of the population feeling discomfort (24°C to 27°C) reduced with -39.9km², -142.3km² and -12.8km² respectively. In the other hand, area with majority of the population anticipated to feel discomfort (27°C to 29°C), area with the entire population feeling thermal discomfort (29°C to 32°C) and area with emergency thermal discomfort conditions (> 32°C) increased with 143.3 Km², 121.7km² and 4km² respectively(See Table 6).

Contrary with observations between 1992-2002, during the dry season between 2002-2012 area with no thermal discomfort (<21°C), area with less than half of the population feeling thermal discomfort

(21 °C to 24°C) as well as area with up to 50% of the population feeling discomfort (24°C to 27°C) appreciated with 17.7km², 65.6 km² and 24.1km² respectively. Area with majority of the population anticipated to feel discomfort (27°C to 29°C), area with the entire population feeling thermal discomfort (29°C to 32°C) and area with emergency thermal discomfort conditions (>32°C) decreased with -29.4km², -45.4km² and -32.8km² respectively(See Table 6).

During the dry season between 2012-2022 area with no thermal discomfort (<21°C), area with less than half of the population feeling thermal discomfort (21 °C to 24°C) as well as area with 50% of the population feeling discomfort (24°C to 27°C) and area with majority of the population anticipated to feel discomfort (27°C to 29°C) decreased with -29km², -105.7km², -86.2km² and -27.1km² respectively. In the other hand, area with the entire population feeling thermal discomfort (29°C to 32°C) and area with emergency thermal discomfort conditions (> 32°C) increased with 15.9km² and 18.7km² respectively (See Table 6).

Table 6. Dry Season Discomfort Index Change Detection from 1992 to 2022 in GKUA

DI	1992 - 2002		2002 - 2012		2012 - 2022	
	Changes Area	%	Changes Area	%	Changes Area	%
<21	-39.9	-5.6	17.7	2.5	-29	-4.2
21 - 24	-142.3	-19.6	65.6	9	-105.7	-14.5
24 - 27	-92.5	-12.8	24.1	3.3	-86.2	-11.9
27 - 29	143.3	20.6	-29.4	-4	-27.1	-3.8
29 - 32	121.7	16.8	-45.4	-6.3	114.9	15.9
>32	4	0.5	-32.8	-4.5	134.8	18.7

Source: Researcher Analysis 2024

Wet Season Discomfort Index Change Detection from 1992 to 2022 in GKUA

During the wet season between 1992-2002, area with less than half of the population feeling thermal discomfort (21 °C to 24°C), area with 50% of the population feeling discomfort (24°C to 27°C), area with the entire population feeling thermal discomfort (29°C to 32°C), area with emergency thermal discomfort conditions (>32°C) decreased with -18.1km², -21.3 km², -1.8 Km² and -15.6km² respectively. In the other hand, area with no thermal discomfort (<21°C) and area with majority of the population anticipated to feel discomfort (27°C to 29°C) and increased with 8.7km² and 48km² respectively (See Table 7). The wet season between 2002-2012 shows that area with

no thermal discomfort (<21°C), area with less than half of the population feeling thermal discomfort (21 °C to 24°C), area with 50% of the population feeling discomfort (24°C to 27°C) and area with majority of the population anticipated to feel discomfort (27°C to 29°C) decreased with -11.8km², -12.8km², -42.6 Km² and -12.4 Km² respectively. In the other hand, area with the entire population feeling thermal discomfort (29°C to 32°C) and area with emergency thermal discomfort conditions (> 32°C) increased with 57.8km² and 21.9km² respectively (See Table 7).

Result at the wet season between 2012-2022 depicts that area with no thermal discomfort (<21°C), area with less than half of the population feeling thermal discomfort (21 °C to 24°C) as well as area with 50%

of the population feeling discomfort (24°C to 27°C), decreased with -52.5 km², -152.5 km² and -74.5km² respectively. In the other hand, area with majority of the population anticipated to feel discomfort (27°C to 29°C), area with the entire population feeling thermal

discomfort (29°C to 32°C) and area with emergency thermal discomfort conditions (> 32°C) increased with 117.2km², 123.7 km² and 36.5 km² respectively (See Table 7).

Table 7. Wet Season Discomfort Index Change Detection from 1992 to 2022 in GKUA

DI	1992 - 2002		2002 - 2012		2012 - 2022	
	Changes Area	%	Changes Area	%	Changes Area	%
<21	8.7	1.2	-11.8	-1.7	-52.5	-7
21 - 24	-18.1	-2.5	-12.8	-1.8	-152.5	-21
24 - 27	-21.3	-2.9	-42.6	-5.9	-74.5	-10.3
27 - 29	48	6.6	-12.4	-1.7	117.2	16.2
29 - 32	-1.8	-0.3	57.8	7.7	123.7	17.2
>32	-15.6	-2.1	21.9	3	36.5	5

Source: Researcher Analysis 2024

Substantially during the dry season, there was an increase in DI between 1992-2002 and 2012-2022 in areas with majority of the population anticipated to feel discomfort, area with the entire population feeling thermal discomfort and area with emergency thermal discomfort conditions increased in GKUA. The DI decreased significantly in area with majority of the population anticipated to feel discomfort, area with the entire population feeling thermal discomfort and area with emergency thermal discomfort conditions increased in GKUA. Obviously during the wet season thermal DI between 1992-2002 was more in areas where majority of the population are anticipated to have thermal discomfort in GKUA while between 2002-2012 and 2012-2022 majority of the population were anticipated to feel discomfort, area with the entire population feeling thermal discomfort and area with emergency thermal discomfort conditions increased in GKUA. It is evident that GKUA is experiencing human thermal discomfort due to rapid urbanization which exacerbate risen LST. This finding agrees with Anwar *et al.* (2022) in their investigation shows that intense urbanization alters the microclimate and ecology of cities by converting naturally vegetated and permeable surfaces into impervious built-up surfaces. These artificial impermeable surfaces re-balance the surface energy budget by storing solar heat due to their higher thermal conductivity, and consequently, increase the LST. The higher the LST in urban area the higher the Human Thermal Comfort (HTC) in GKUA of Nasarawa State.

4. Conclusion

This study ascertain the Effect of Land Use/Land Cover Changes on Land Surface Temperature and

Human Thermal Comfort in Greater Karu Urban Area of Nasarawa State, Nigeria. Substantially during the dry season, there was an increase in DI between 1992-2002 and 2012-2022 in areas with majority of the population anticipated to feel discomfort, area with the entire population feeling thermal discomfort and area with emergency thermal discomfort conditions increased in GKUA. The DI decreased significantly in area with majority of the population anticipated to feel discomfort, area with the entire population feeling thermal discomfort and area with emergency thermal discomfort conditions increased in GKUA. Obviously during the wet season thermal DI between 1992-2002 was more in areas where majority of the population are anticipated to have thermal discomfort in GKUA while between 2002-2012 and 2012-2022 majority of the population were anticipated to feel discomfort, area with the entire population feeling thermal discomfort and area with emergency thermal discomfort conditions increased in GKUA.

Recommendations

Given the finding of the study the following recommendations were made. Implement integrated urban planning through zoning regulations and smart growth policies. Enhance green infrastructures through urban greening and green roofs and walls. Adoption of cool and sustainable building materials that have high reflective capacities. Promote sustainable land management systems by designing land use plans that prioritize natural land cover and minimize disturbance of existing ecosystems. There should be towards restoring degraded areas and implementing land management practices that enhance natural vegetation and biodiversity. Develop and implement

comprehensive climate action plans that address urban heat islands and integrate strategies for improving thermal comfort. Establish regulations and monitoring systems to ensure adherence to environmental and building codes that promote sustainability. There is need to leverage on remote sensing and GIS to consistently monitor changes in land use/land cover and their impact on LST and thermal comfort.

5. References

1. Adakayi, P.E. and Ishaya S. (2016). Assessment of Minimum Temperature in some parts of Northern Nigeria. *Ethiopian Journal of Environmental Studies and Management*. 9(2): 220-227. Department of Geography and Environmental Studies Bahir Dar University, Ethiopia. Available online at <http://www.ajol.info/index.php/ejesm>.
2. Ade, M. A. and Afolabi, Y. D. (2013). Monitoring Urban Sprawl in the Federal Capital Territory Of Nigeria Using Remote Sensing And Gis Techniques. *Ethiopian Journal of Environmental Studies and Management*. 6 (1), 82-95.
3. Adeyeri, O. E., Akinsanola, A. A., &Ishola, K. A. (2017). "Investigating urban heat island characteristics over Abuja, Nigeria: Relationship between land surface temperature and multiple vegetation indices", Remote Sensing Applications: Society and Environment.
4. Anwar Hossain, H. M. Imran, MahaadIssaShammas, Mohan Kumar Dasc, Md. RabiulIslama, KalimurRahmand and Mansour Almazroui (2022). Land surface temperature and human thermal comfort responses to land use dynamics in Chittagong city of Bangladesh. *Geomatics, Natural Hazards and RIS*. 13(1), 2283–2312 <https://doi.org/10.1080/19475705.2022.2114384>
5. Audu, E.B., Abubakar, A.S., Ojoye, S., Muhammed, M., & Mohammed, S. Y. (2018). Characteristics of annual rainfall over Guinea Savanna Zone, Nigeria. *Journal of Information, Education, Science and Technology (JIEST)*, 5(1), 87- 94.
6. Balogun A. I., Debo. Z. Adeyewa, Ahmed. A. Balogun and Tobi. E. Morakinyo (2011). Analysis of urban expansion and land use changes in Akure, Nigeria, using remote sensing and geographic information system (GIS) techniques. *Journal of Geography and Regional Planning*. 4(9), 533-541.
7. Chen Y, Yang J, Yu W, Ren J, Xiao X and Xia J C (2023). Relationship between urban spatial form and seasonal land surface temperature under different grid scales Sustain. *Cities Soc*. 89, 104374.
8. Choudhury D, Das K, Das A. (2019). Assessment of land use land cover changes and its impact on variations of land surface temperature in Asansol-Durgapur Development Region. *Egypt J Remote Sens Space Sci*. 22(2): 203–218.
9. Ejaro, S. and Abubakar, A. (2013). Impact of Rapid Urbanization on Sustainability Development of Nyanya, Federal Capital Territory, Abuja, Nigeria. *Journal of Social Science and Management*, 3, 31-44. <https://doi.org/10.4314/jasem.v17i2.13>
10. Giannaros T M, Melas D, Daglis I A, Keramitsoglou I. (2014). Development of an operational modeling system for urban heat islands: an application to Athens, Greece. *Nat Hazards Earth Syst Sci*. 14(2):347–358.
11. Imran H M, Anwar Hossain, A. K. M. Saiful Islam, Aatur Rahman, MdAbulEhsanBhuiyan, Supria Paul and AkramulAlam (2021). Impact of Land Cover Changes on Land Surface Temperature and Human Thermal Comfort in Dhaka City of Bangladesh. *Earth Systems and Environment*. 2021(5), 667–693. <https://doi.org/10.1007/s41748-021-00243-4>
12. HimanshuGovil and SubhanilGuha (2021), A seasonal relationship between land surface temperature and normalized difference bareness index. *South African Journal of Geomatics*. 10(2), 13-21. DOI: <http://dx.doi.org/10.4314/sajg.v10i2>.
13. Hou H, Wang R, Murayama Y. (2019). Scenario-based modelling for urban sustainability focusing on changes in cropland under rapid urbanization: A case study of Hangzhou from 1990 to 2035. *Sci. Total Environ*. 661:422–431. doi: 10.1016/j.scitotenv.2019.01.208.
14. Ishaya, S. (2020). Assessment of Urban Generated Climate Anomaly in Okene Town, Okene Local Government Area of Kogi State, Nigeria. *FUDMA Journal of Sciences (FJS)*. 4(2): 101-110. DOI: <https://doi.org/10.33003/fjs-2020-0402-203>
15. Ishaya S. and Areo, Isaac Olajide (2018). Assessment of ofLanduse/Landcover change in Kwali Area Council UsingGeo-Informatic Techniques. *The Environmental Studies (A Multidisciplinary Journal)*. 1(1)2: 38-47.
16. Kumar, S and Sangwan R S (Urban Growth, Land Use Changes and Its Impact on Cityscape in Sonipat City Using Remote Sensing and GIS Techniques, Haryana, India. *International Journal of Advanced Remote Sensing and GIS*. 3(4). 24-31.
17. Lee Bak Yeo, Gabriel HohTeck Ling, Mou Leong Tan, and Pau Chung Leng (2021): Interrelationships between Land Use Land Cover (LULC) and Human Thermal Comfort (HTC): A Comparative Analysis of Different Spatial Settings.
18. Mumtaz F, Tao Y, de Leeuw G, Zhao L, Fan C, Elnashar A, Bashir B, Wang G, Li L, Naeem S, Wang D. (2020). Modelingspatio-temporal land transformation and its associated impacts on land surface temperature (LST). *Remote Sens*. 12(18):2987. doi: 10.3390/rs12182987.

19. NASA (2011). Landsat 7 Science Data Users Handbook (United States). Retrieve 2024 from <http://ltpwww.gsfc.nasa.gov/IAS/handbook/handbooktoc.html>
20. Olubukola Catherine Obateru, Sunday Ishaya, Esemuze Lucky, Peter E. Adakayi (2023). Spatio-Temporal Occurrence of Climate Change: Evidence from Rainfall and Temperature Records in the Agro-Ecological Zones of Ondo State, Nigeria. *World Scientific News*182: 237-249.
21. Ren J, Yang J, Zhang Y, Xiao X, Xia J C, Li X and Wang S (2022). Exploring thermal comfort of urban buildings based on local climate zones. *J. Clean. Prod.* 340, 130744.
22. Rikko, S. Laraba and Laka I. Shola (2013). Monitoring Urban Sprawl in Greater Karu Urban Area (Gkua), Nasarawa State, Nigeria. *Journal of Environment and Earth Science.* 3(13), 24-32. ISSN 2224-3216
23. Thani, S.K.S.O.; Mohamad, N.; Jamaludin, S. Outdoor Thermal Comfort (2013): The Effects of Urban Landscape Morphology on Microclimatic Conditions in a Hot-Humid City. *WIT Trans. Ecol. Environ*, 179, 651–662.
24. Udeh, A.U. (2010). Impact of Development of the Federal Capital City, Abuja on Selected Settlements in Karu Local Government Area, Nasarawa State, Nigeria. *Journal of Service Science and Management*, 12(5), 34-51.
25. Zhang Y and Liang S. (2019). Impacts of land cover transitions on surface temperature in China based on satellite observations. *Environ Res Lett.* 13(2):024010.